

Analysis of weld pool vibration characteristics in pulsed gas metal arc welding

Lü Xiaoqing^{1,2}, Zhang Peng^{1,2}, Shen Jun^{1,2}

吕小青, 张鹏, 沈俊

1. School of Materials Science and Engineering, Tianjin University, Tianjin 300072, China;

2. Tianjin Key Laboratory of Advanced Joining Technology, Tianjin University, Tianjin 300072, China

Received 9 July 2019; accepted 18 October 2019

Abstract Using highspeed camera image measuring and processing, the contour of the weld pool was extracted accurately in pulsed metal inert gas (P-MIG) welding. Based on this extraction method, time and frequency domain characteristics at different points along the contour of the weld pool were analyzed for one pulse one droplet and one pulse two droplets, respectively. The results show that, because of the wave super position that was created by the pulsed arc and droplet impacting the weld pool, the oscillation amplitude along the weld pool fluctuated and decreased with an increase in distance from the point to the arc center. The oscillation near the arc center was complex and intense for one pulse two droplets, and the amplitude were relatively small because the oscillation caused by the pulsed arc could be offset by the molten droplet impact. The weld pool oscillation that was caused by the pulsed arc was stronger than that caused by the droplet.

Key words pulsed metal inert welding, weld pool oscillation, interference, time domain chart, frequency domain chart

0 Introduction

The weld pool oscillation is a direct reflection of the weld process stability; thus many related research reports exist to describe this phenomenon and it has received much attention since the 1990s. For example, to analyze the relationship between the weld formation and natural oscillation frequency, references[1 – 3] investigated TIG weld pool oscillation through a trial test and numerical simulation, respectively. For another, some research exists on the oscillation modes^[4 – 5]. However, most current studies focus on TIG welding, and few studies have focused on MIG welding^[6 – 9]. Because the MIG weld pool can be affected easily by the droplets, the oscillation process is more complex, which makes the natural oscillation frequency more difficult to obtain. Thus, it is necessary to recognize and understand the oscillation process from a new perspective. In this paper, with high speed photography and image processing techno-

logy, the variation laws of the P-MIG weld pool oscillation can be obtained by analyzing the time and frequency domain properties, which can help to establish the primary theoretical basis for further investigation of the relationship between the weld pool oscillation and weld formation.

1 Experimental method

Fig. 1 shows the experimental apparatus, including the welding source system, highspeed camera acquisition system and electrical signals acquisition system. The welding system consisted of a LINCOLN welding machine (V350) and a matching wire feeder. The highspeed camera acquisition system consisted of a highspeed camera (FASTCAM-Super10KC) and a backlight source (xenon lamp)^[10]. The acquisition frequency was set to 2kHz, and the resolution was 256 × 120 pixels. The electrical signals acquisition system comprised a voltage sensor, a current sensor, a working

Foundation item: This work was supported by the National Natural Science Foundation of China (Grant Numbers 51205283).

Corresponding author: Lü Xiaoqing, (1978 –), Doctor, Professor. Mainly engaged in welding inverter and automation, arc welding chaos theory and arc welding process research. E-mail: xiaoqinglv77@163.com

doi: 10.12073/j.cw.20190709002

computer and Labview software. The 1.2-mm diameter welding wire type was H08Mn2SiA. In this experiment, two welding procedures, including one pulse one droplet and

one pulse two droplets were performed on 10-mm thick mild steel. The detailed welding parameters are shown in Table 1.

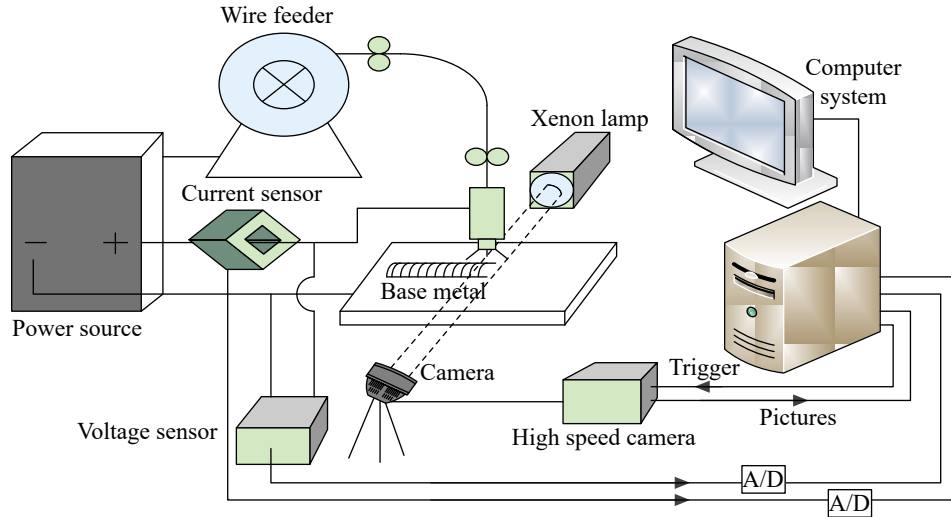


Fig. 1 Schematic of welding experimental system

Table 1 Welding parameters

Welding method	Peak current I_p/A	Base current I_b/A	Duty circle $D(\%)$	Pulse frequency f/Hz	CTWD d/mm	Wire feed speed $V_f/(m \cdot min^{-1})$	Welding speed $V_w/(mm \cdot s^{-1})$
One pulse one droplet	410	60	45	80	20	3.8	3.0
One pulse two droplets	240	60	45	20	20	4.0	4.5

2 Weld pool image processing

2.1 Extraction of weld pool contour

Because of the strong arc in the P-MIG process, a composite filter system and backlight source were applied to eliminate the disturbance from the arc. The quality of the raw high speed images was poor and the weld pool contour was indistinct because of the welding fumes. Thus, it is essential to extract the clear weld pool contour to obtain the time domain chart of the weld pool oscillation and frequency domain chart with a Fourier transform method. By using the image-processing technique based on MATLAB, a clear weld pool contour could be obtained from the raw images. The detailed process procedure can be divided into four steps: (1) raw images (Fig. 2a) de-noise processing based on gray transformation and median-smooth filtering methods (Fig. 2b); (2) contour extracting based on logarithm function (Fig. 2c); (3) removing useless noise points at relatively low pixels (Fig. 2d); (4) excising the interference from welding wire, droplets and a strong arc to obtain final images that only include the weld pool contour (Fig. 2e)^[11–12].

2.2 Analysis of weld pool oscillation

As mentioned previously, through MATLAB, the processed images are saved in pixel format, and thus, each pixel size is 0.1 mm according to the wire diameter and corresponding number of the pixels. As shown in Fig. 2, the welding torch and highspeed camera remained stationary, and the welded workpiece moved to the right, therefore, the melted pool was located near the right of the arc center. If we consider that the wave travelled along all directions in the weld pool, then a horizontal oscillation existed vertical to the welding direction. The width of the weld pool was so narrow that the highspeed camera could not capture the horizontal oscillation; the longitudinal oscillation has been discussed in our research. The top-left corner of the image was set as the origin (0,0) of the coordinates, the moving direction of the workpiece was set as the x -axis, and the direction vertical to the x -axis was set as the y -axis. For the processed weld pool contour in each image (Fig. 2e), the variation of y -axis values with time on fixed values of x was investigated, which was used to obtain the oscillatory changes of the weld pool contour.

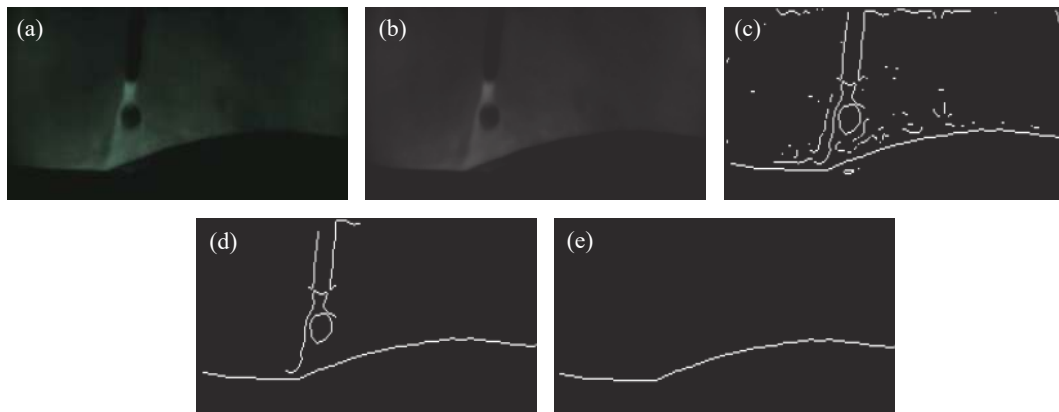


Fig. 2 Weld pool contour extracting (a) Raw images (b) Gray transformation and median-smooth filtering (c) Contour extracting (d) Removing useless noise points (e) Image simplification

3 Experimental results and discussion

To study the oscillatory characteristics of the weld pool, two typical transition modes of one pulse one droplet and one pulse two droplets during P-MIG welding were compared and discussed. The pulsed frequency of one pulse one droplet was 80 Hz, and the pulsed frequency of one pulse two droplets was 20 Hz. Every 10 pixels (equal to 1 mm) in the x -axis direction on the weld pool contour was taken as one point for the weld pool oscillation analysis.

3.1 One pulse one droplet

In Fig. 3, several pixel points with different distances (27, 37, 47, 57, 67, 77 pixels) from the arc center were selected for the one pulse one droplet during the P-MIG process. The specified coordinate point (96,97), namely, the arc center, was the projection point of the arc column axis on the weld pool. Fig. 4a and Fig. 4b show the time and frequency domain charts of the oscillation, respectively. In Fig. 4a, the pixel height (y -axis) in the time domain represents the pixel variation of the weld pool contour points over time along the y -axis. Fig. 4b shows the amplitude distribu-

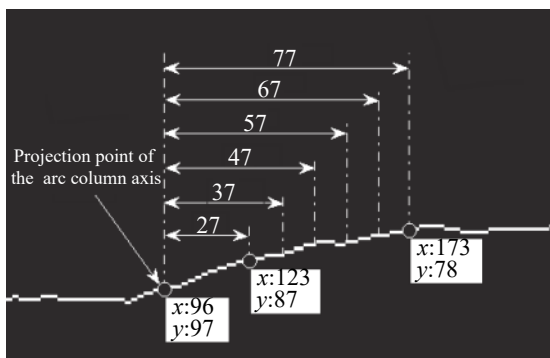


Fig. 3 Point selection along the weld pool contour

tion trend of several points a distance (27–77 pixels) away from the arc center.

From the time domain charts, the actual amplitudes of different points on the weld pool contour were different. As shown on the frequency domain charts, all points can reach a maximum amplitude of 80 Hz. This maximum occurred because the pulsed frequency was identical to the droplet-transition frequency, and the maximum amplitude was their superposition. The secondary maximum amplitude was 160 Hz, which was caused by a second harmonic. Compared with the maximum amplitudes of different frequency domain charts, it was obvious that the pixel amplitude distances away from arc center (27, 47, 57 pixels) were higher, whereas the amplitude of pixel 37 was lower, and the amplitudes of pixels 67 and 77 were the lowest. The amplitude characteristics of the frequency domain were consistent with that of the time domain. Far from the arc center, the maximum amplitude decreased initially and then increased, and it decreased again gradually and increased finally.

In the transition mode of one pulse one droplet, the current pulse frequency was 80 Hz. In each pulse cycle, the pulsed arc and molten droplets acted on the molten pool successively, which is equivalent to generating two kinds of “oscillatory stimulations” on the molten pool under the action of forces. Far from the arc center, the molten pool had solidified with a decrease in liquid metal, which resulted in a weaker gravity and inertia force. The viscosity and rigidity both increased accordingly, and the pool metal oscillated with a lower amplitude in the form of a solid approximately. Therefore, the overall trend of weld pool oscillation weakened gradually during welding. When two kinds of travelling waves that were caused by the pulsed arc and molten droplets spread far away, they could overlap easily and interfere, which led to an enhanced oscillation on some points and a weakened oscillation on other points. With an

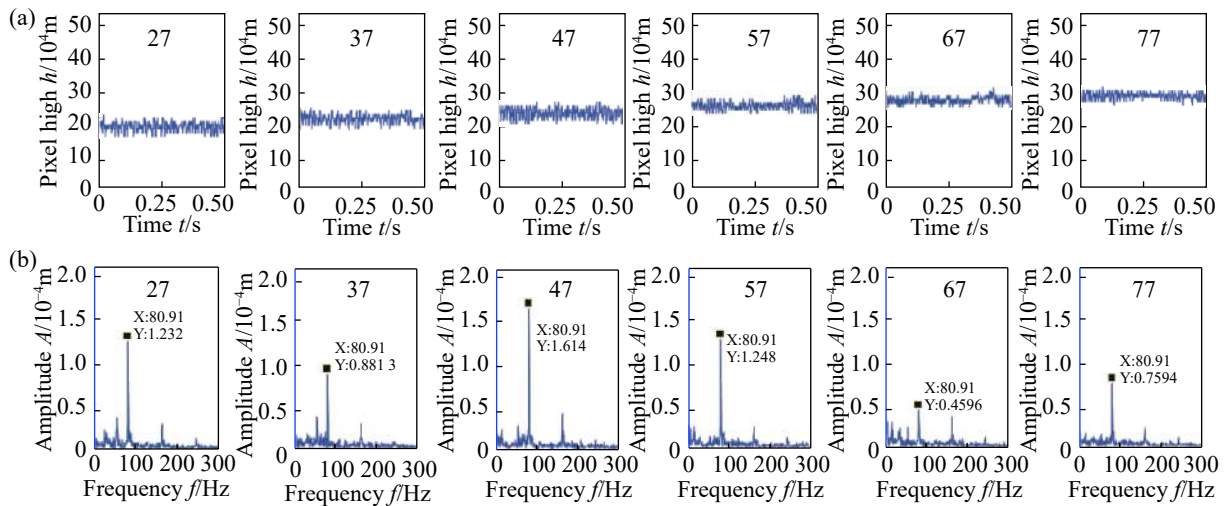


Fig. 4 Vibration images of one pulse one droplet (a) Time domain chart (b) Frequency domain chart

increase distance from the arc center, the amplitudes of different points on the weld pool contour presented a fluctuating decreasing trend instead of a linear decrease.

3.2 One pulse two droplets

To distinguish the effect of pulsed arc and molten droplets on the weld pool, the transition mode of one pulse two droplets was selected. The detailed welding parameters are shown in Table 1, the pulse frequency was 20 Hz and the transition frequency was 40 Hz. The selected principle of weld pool contour points under one pulse two droplet transfer is the same as one pulse one droplet. The time and frequency domain charts of the weld pool oscillation are shown in Fig. 5a and Fig. 5b. The distances from the arc center were 16, 26, 36, 46, 56, 66 and 76 pixels in sequence from left to right in each image. As shown in Fig. 5a, the amplitudes of the some points were larger and other points

were smaller. The oscillation near the arc center was more complicated and intensive than further from the center. According to Fig. 5b, all points could reach the maximum amplitude of 20 Hz, and the weld pool oscillation that was caused by the pulsed arc presented a fluctuating transmission form. Except for 20 Hz, there existed a secondary maximum amplitude of 40 Hz, which was caused mainly by the metal transfer and second harmonic. It was difficult to capture the secondary maximum amplitude as the distance from the arc center increased. The weld pool oscillation that was caused by the molten droplet presented a fluctuating transmission form with an overall decreasing trend.

In the one pulse two droplets experiments, the pulse frequency of the current was 20 Hz, and the pulsed arc and molten droplets acted on the molten pool successively, to stimulate the weld pool oscillation. Different kinds of waves in the weld pool are caused by the pulsed arc and droplets

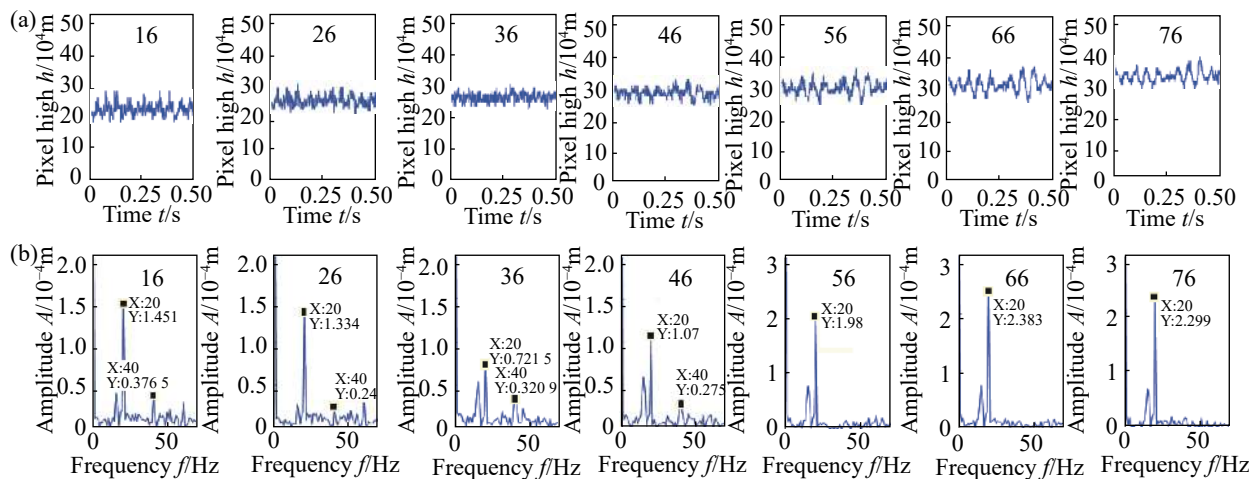


Fig. 5 Vibration images of one pulse two droplets (a) Time domain chart (b) Frequency domain chart

and these could overlap and interfere with each other, which results in variable amplitudes of each point. Because the impact force of the pulsed arc on the weld pool was larger than that of the droplets, the peak value of 20 Hz that was caused by the pulsed arc appeared in each frequency domain chart. In contrast, the spread distance of the weld pool oscillation that was caused by the droplets was limited. Therefore, it is more complicated and intensive near the arc center in the time domain chart. The frequency domain contained the peak value of 20 Hz that was caused by the pulsed arc, and contained the peak value of 40 Hz that was caused by the droplets and second harmonics. Only the peak value of 20 Hz existed far from the arc center. However, the amplitudes of the time and frequency domain charts were lower near the arc center because oscillations that were caused by the pulsed arc are offset by droplet impact.

For the transfer mode of the multiple pulses one droplet, the pulsed arc and droplet transfer were not accomplished in each pulse cycle and several waves prevented them from being superposed directly. Therefore, multiple pulses one droplet mode was not discussed in this study.

4 Conclusion

(1) The P-MIG weld pool oscillation characteristics of one pulse one droplet and one pulse two droplets were compared and discussed. The generation of weld pool oscillation resulted from wave superposition that was created by pulsed arc and droplet impact on the weld pool. An increase in distance from the arc center made it more difficult to generate a weld pool oscillation with a lower weld pool temperature and a larger viscosity. Therefore, the amplitude variation of the weld pool contour presented an overall fluctuating decreasing tendency.

(2) The oscillation near the arc center was complex and intense for one pulse two droplets and the amplitude was relatively small because the oscillation that was caused by the pulsed arc could be offset by the droplet. Because the weld pool oscillation that was caused by the pulsed arc was stronger than that by the droplet, the weld pool oscillation was caused only by the pulsed arc far from the arc center.

References

- [1] Xiao Y H, Ouden G D. A study of GTA weld pool oscillation. *Welding Journal*, 1990, 69(8):289 – 293.
- [2] Andersen K, Cook G E, Bamett R J, et al. Synchronous weld pool oscillation for monitoring and control. *IEEE Transactionson Industry Applications*, 1997, 33(2):464 – 471.
- [3] Liu W, He J S, Wu Q S, et al. Numerical simulation of effect of arc force on shape of liquid surface of TIG weldingmolten pool. *Transactions of the China Welding Institution*, 2007, 28(7):69 – 71. (in Chinese)
- [4] Xiao Y H, Ouden G D. Weld pool oscillation during GTA weldingof mild steel. *Welding Research Supplement*, 1993, 72(8):428 – 434.
- [5] Maruo H, Hirata Y. Natural frequency and oscillation modes ofweld pool. *Welding International*, 1993, 7(8):614 – 619.
- [6] Wang L L, Lu F G, Cui H C, et al. Investigation of molten pool oscillation during GMAW-P process based on a 3D model. *Journalof Physics D: Applied Physics*, 2014, 47(46):204 – 217.
- [7] Ramos E G, Carvalho G C D, Alfaro S C A. Analysis of weld pool oscillation in GMAW-P by means of shadowgraphy imageprocessing. *Welding International*, 2015, 29(3):197 – 205.
- [8] Matsui H, Chiba T, Yamazaki K. Detection and amplification ofthe molten pool natural oscillation in consumable electrode arcwelding. *Welding International*, 2014, 28(1):5 – 12.
- [9] Zhao P C, Liang Y, Ma S S. Numerical simulationon wave behaviors at a weld pool free surface in pulse gas metalarc welding. *Journal of Qingdao University of Science andTechnology*, 2013, 34(4):407 – 413.
- [10] Yang Y Q, Li H, Li J Y, et al. High-speed photography with multi-information synchronizer for GMAW. *Transactions of the China Welding Institution*, 2002, 23(6):29 – 32. (in Chinese)
- [11] Zhou P, Li X D. *MATLAB digital image processing*. Beijing: Tsinghua University Press, 2012.
- [12] Yang Q, Wang G W, Hua X M, et al. Edge detection of metal transfer image based on wavelet transform. *Transactions of the China Welding Institution*, 2007, 28(4):38 – 40. (in Chinese)